

## **Supporting Information:**

### **Amyloid $\beta$ -Protein Assembly: Differential Effects of the Protective A2T Mutation and the Recessive A2V Familial Alzheimer's Disease Mutation**

Xueyun Zheng,<sup>†</sup> Deyu Liu,<sup>†</sup> Robin Roychaudhuri,<sup>‡</sup> David Teplow<sup>‡</sup> and Michael T. Bowers<sup>†\*</sup>

<sup>†</sup>Department of Chemistry and Biochemistry, University of California, Santa Barbara, CA 93106, United States

<sup>‡</sup>Department of Neurology, David Geffen School of Medicine, Molecular Biology Institute and Brain Research Institute, University of California Los Angeles, Los Angeles, CA 90095, United States

\*To whom correspondence should be addressed: bowers@chem.ucsb.edu; Tel.: 805-893-2893; Fax: 805-893-8703.

## **Injection energy study for A2T and A2V A $\beta$ 42**

To assign the peaks in the ATDs unambiguously and better understand the oligomer distributions for A $\beta$ 42 mutants, the ATDs for A $\beta$ 42 mutants were measured at different injection energies. Injection energy varied from ~20 to 150 eV can be applied before the ions are injected into the drift cell for ion mobility separation. At low injection energy, the ions are rapidly thermalized by cooling collisions with the helium gas in the drift cell and therefore large complexes can be preserved through the process. At high injection energy, the ions are given energy that can lead to internal excitation which can cause isomerization into low energy structure or dissociation of large noncovalent complexes into smaller species.

The ATDs of -5/2 A2T and A2V A $\beta$ 42 are recorded under different injection energies and shown in Figure S1. As shown in middle panel, the ATD recorded at an intermediate injection energy (40 eV) displays three features which are assigned as dimer, tetramer and hexamer, where the intensities of hexamer and tetramer features are comparable. When the injection energy is lowered to 25 eV (Figure S1 top panel), the hexamer feature increases and becomes even more dominant while the tetramer and dimer features are decreased. However, there is still no feature with lower arrival times observed, suggesting there is no dodecamer or larger oligomer formation. When applied with a high injection energy (100 eV, Figure S1 bottom panel), the hexamer feature disappears while the tetramer and dimer become dominant features, which suggests the hexamer species were dissociated into smaller oligomers.

The ATDs of z/n = -2 A $\beta$ 42 mutants were measured at different injection energies to better understand their oligomer distributions and the data are shown in Figure S2. As shown in Figure S2a, the trimer feature in the ATD of -2 A2T A $\beta$ 42 under lower injection energy (25 eV) does not increase compared to that under injection energy of 40 eV and the trimer feature disappears

when applied with high injection energy (100 eV). However, the trimer feature of the  $z/n = -2$  A2V A $\beta$ 42 increases significantly when applied with lower injection energy (see Figure 2b). This suggests that the trimer formation is more favored for A2V than A2T A $\beta$ 42.

The injection energy study of the  $-8/3$  A2V A $\beta$ 42 (Figure S2c) shows that when applied with lower energy (25 eV), the hexamer feature increases and the trimer peak gets sharper which suggests there are more hexamers preserved. When applied with high energy (100 eV), the hexamer feature disappears and the broad trimer feature becomes dominate peak.

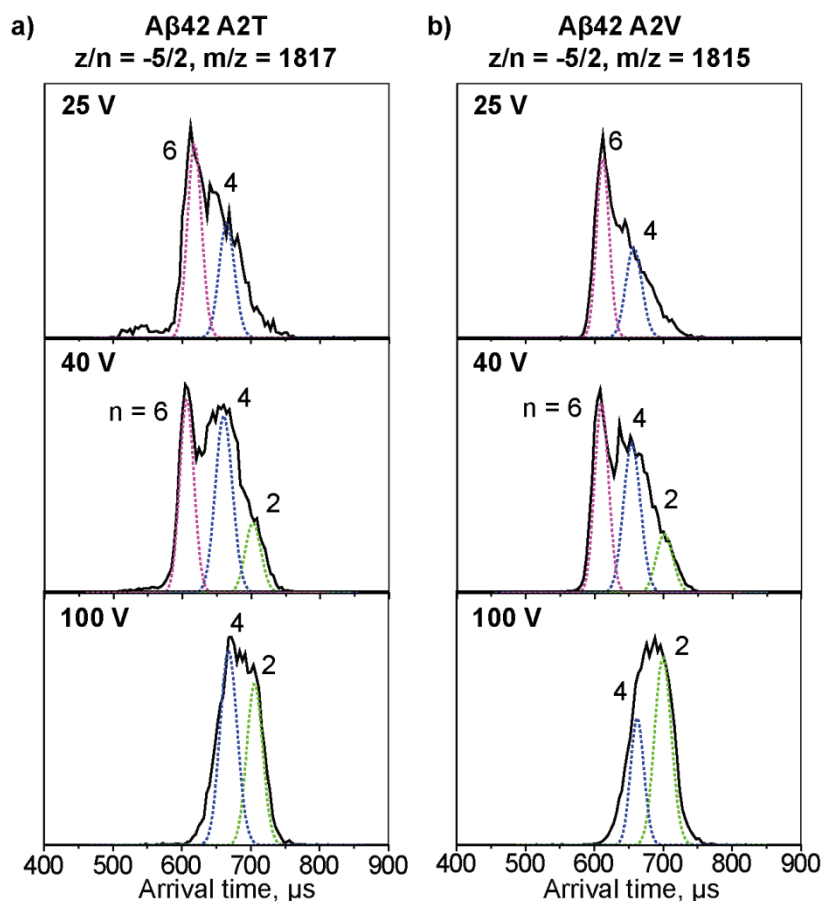


**Figure S1.** ATDs for  $z/n = -5/2$  peaks for a) A $\beta$ 42 A2T and b) A $\beta$ 42 A2V under different injection energies. The oligomer order ( $n$ ) is noted for each feature. The dashed lines represent the peak shape for a single conformation.

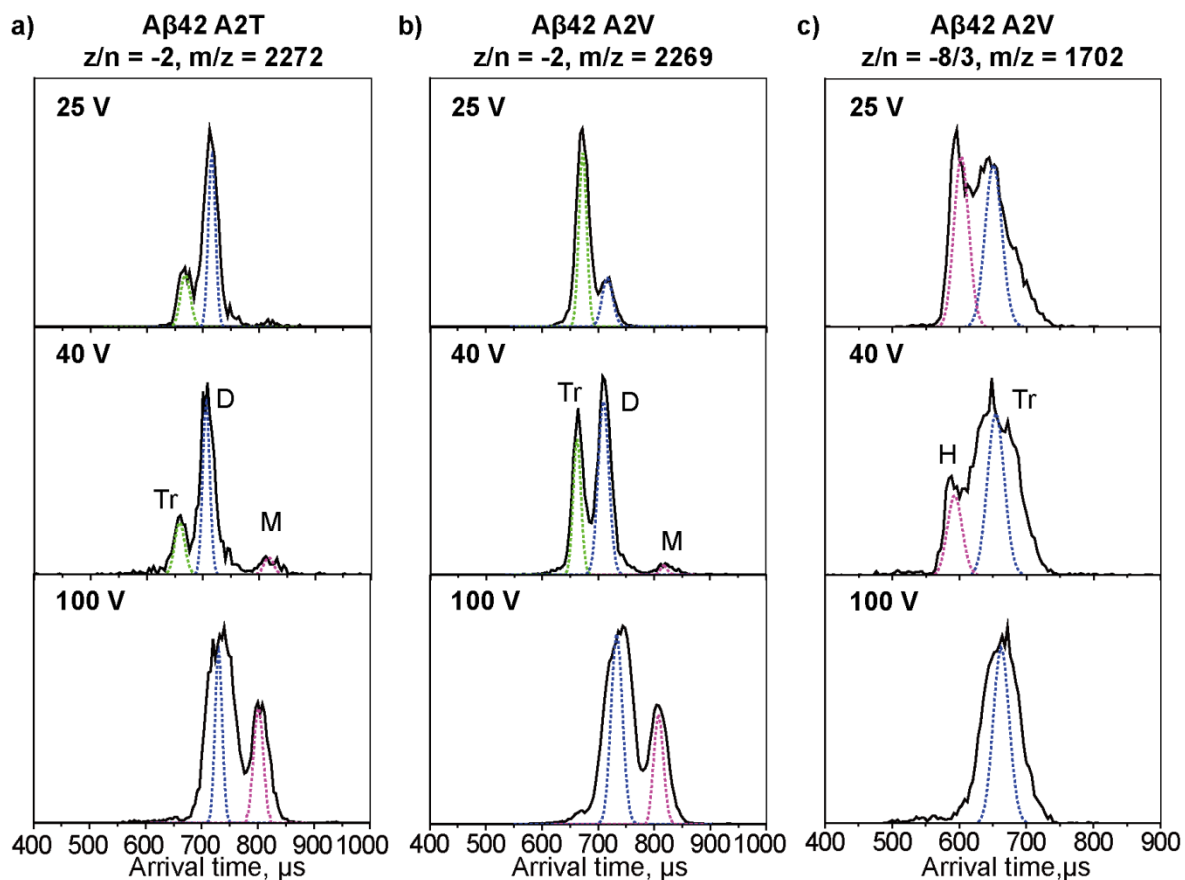


**Figure S2.** ATDs for  $z/n = -2$  peaks for a) A2T A $\beta$ 42, b) A2V A $\beta$ 42 and c)  $z/n = -8/3$  peak for A2V A $\beta$ 42 under different injection energies. The oligomer order is noted for each feature where M represents monomers, D represents dimer and Tr represents trimers, H represents hexamer. The dashed lines represent the peak shape for a single conformation.

### Assignment of possible pentamer peak for A2V A $\beta$ 42

The mass spectrum of A2V (Figure 3Sa) shows one additional peak between  $z/n = -4$  and  $-3$  which would be assigned as  $-17$  pentamer. To confirm this peak assignment unambiguously, an ATD of this possible  $-17/5$  peak was recorded and shown in Figure 3Sb. The ATD shows only one feature with arrival time at  $\sim 590 \mu\text{s}$  and the experimental cross section for the monomer in the pentamer measured from this peak is  $\sigma/n = \sim 685 \text{ \AA}^2$ . When compared to the cross section of monomer obtained from other oligomers from dimer to hexamer ( $\sigma/n = 491\text{-}626 \text{ \AA}^2$ ), the cross section for this pentamer is significantly larger which is very unlikely to be true as the peptide assembly often involves intermolecular interactions which results in a smaller conformation. Secondly, this assumed pentamer carries 17 charges which distribute more than 3 charges on one monomer in the complex. From the table (Figure 3Sc), we can see that even hexamer carries only 15 charges and others pick up less than 3 charges for each monomer in the complexes (2-2.5 charges). Therefore it is very unlikely this peak is a real pentamer peak. Taken together, no pentamer of A2V A $\beta$ 42 is observed from our ion mobility study.

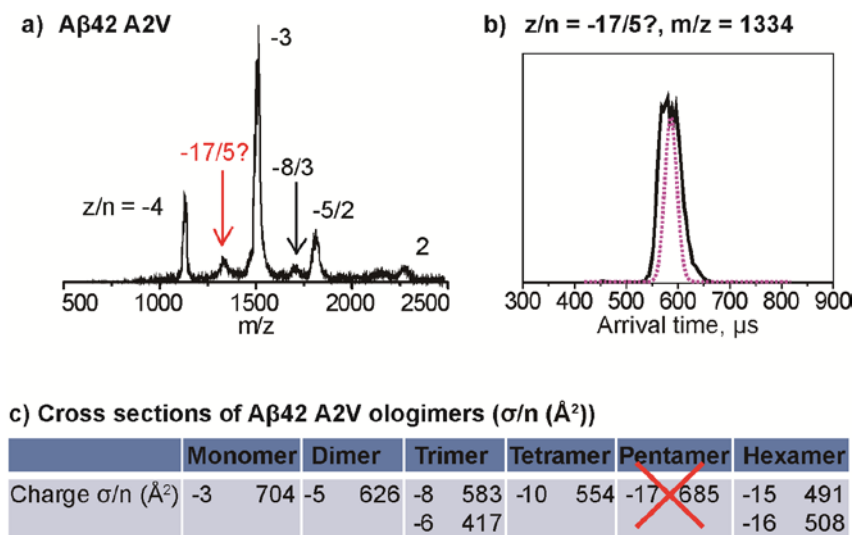


**Figure S3.** Assignment of  $-17/5$  peak for A2V A $\beta$ 42. a) Mass spectrum of A2V A $\beta$ 42. The charge state of each species is noted with  $z/n$ , where  $z$  is the charge and  $n$  is oligomer number. b)

ATD of  $z/n = -17/5$  peaks for A2V A $\beta$ 42. c) Cross sections of A2V A $\beta$ 42 oligomers, the error for each cross section is within 1%.

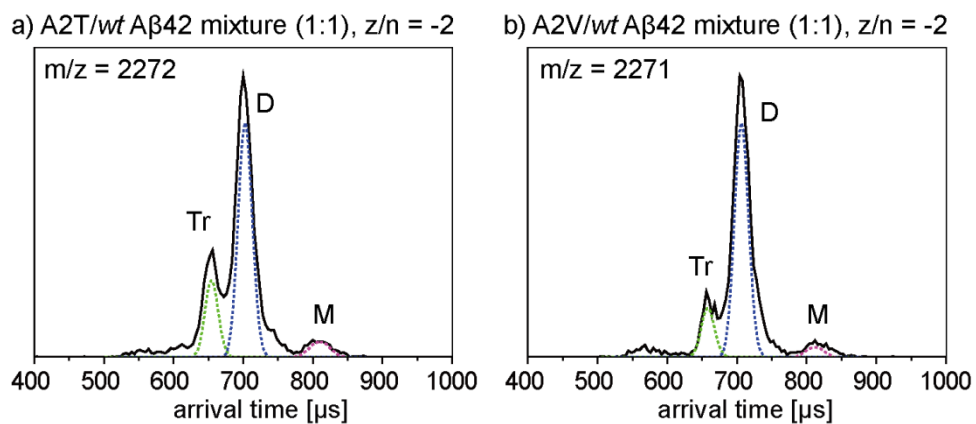


**Figure S4.** ATDs of  $z/n = -2$  for the A2T/wt and A2V/wt A $\beta$ 42 mixtures. The oligomer order is noted for each feature where M represents monomers, D represents dimer and Tr represents trimers. The dashed lines represent the peak shape for a single conformation. The injection energy in panels a, and b is 40 eV.

## The effects of A2T mutant on early assembly of *wt* A $\beta$ 40

Ion mobility studies of an equimolar mixture of A2T and *wt* A $\beta$ 40 were performed and the results are shown in Figure S5. The mass spectrum of *wt*/A2T A $\beta$ 40 mixture (Figure S5a) shows four sets of peaks corresponding to  $z/n = -4, -3, -5/2$  and  $-2$  charge states. The ATDs of the  $-5/2$  oligomer peaks (Figure S5b, c and d) show two features with arrival times at  $\sim 710$  and  $670$   $\mu\text{s}$ , which can be assigned as *wt*/A2T homo- or hetero-dimers, tetramers, based on their cross sections. This result is consistent with the results of the *wt*/A2T A $\beta$ 42 mixture that A2T inhibits the formation of *wt* A $\beta$ 42 dodecamer and that A2T mutation protects against AD and protects against the cognitive decline in the elderly without AD.

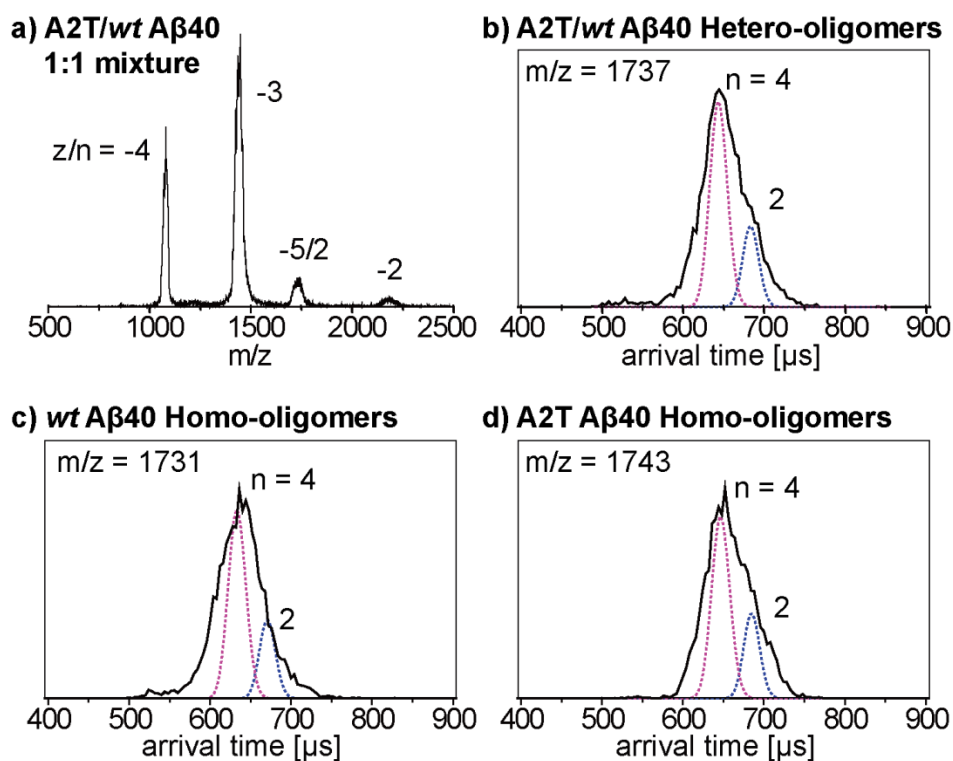


**Figure S5.** Ion mobility study of an equimolar mixture of A $\beta$ 40 *wt* and A2T mutant. a) Mass spectrum of A $\beta$ 40 A2T/*wt* mixture. b-d) ATDs of three  $-5/2$  oligomer peaks. The oligomer order ( $n$ ) is noted for each feature. The injection energy in panels b, c, and d is 40 eV.

## The effects of A2V mutant on early assembly of *wt* A $\beta$ 40

Ion mobility studies of an equimolar mixture of A2V and *wt* A $\beta$ 40 were performed and the results are shown in Figure S6. The mass spectrum of A $\beta$ 40 *wt*/A2V mixture (Figure S6a) shows four sets of peaks corresponding to  $z/n = -4, -3, -5/2$  and  $-2$  charge states. The ATDs of the  $-5/2$  oligomer peaks all display two features with arrival times at  $\sim 710$  and  $670$   $\mu\text{s}$ , which can be assigned as *wt*/A2V A $\beta$ 40 homo- or hetero-dimers, tetramers and no larger oligomers especially hexamers and dodecamers are observed. These results indicate that A2V mutant forms small hetero-oligomers (hetero-dimer and tetramers) with *wt* A $\beta$ 40 and inhibits the formation of A2V A $\beta$ 40 hexamer or dodecamer. This is consistent with the results of *wt*/A2V A $\beta$ 42 mixture that A2V inhibits dodecamer formation and explains the physiology fact that heterozygous carrier of A2V mutation does not develop early-onset of AD.

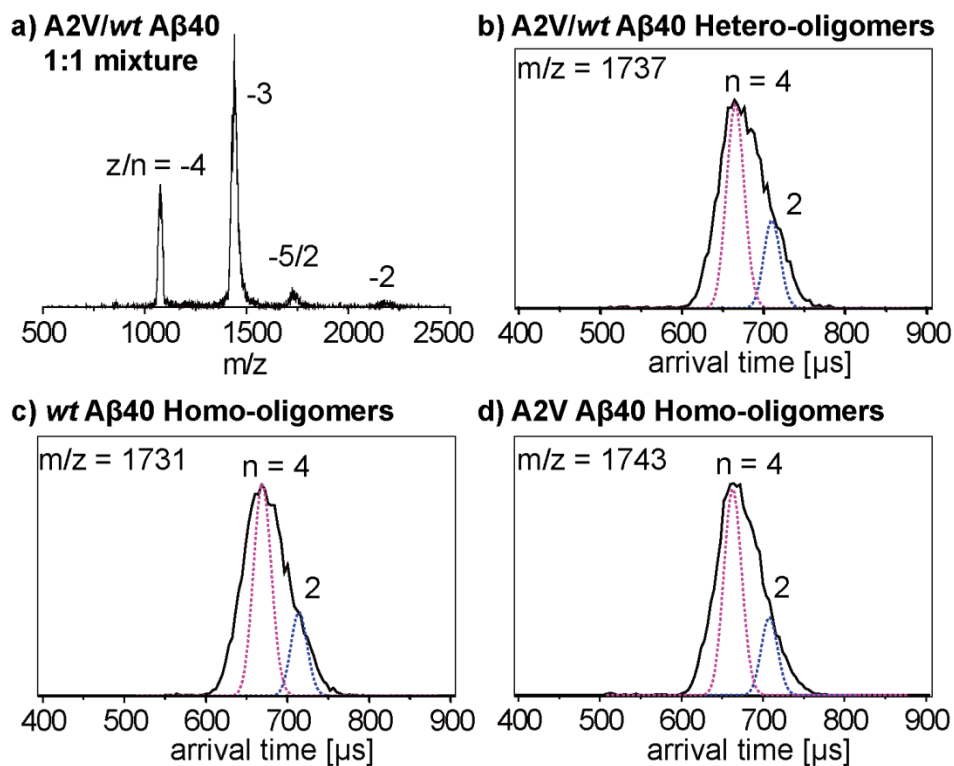
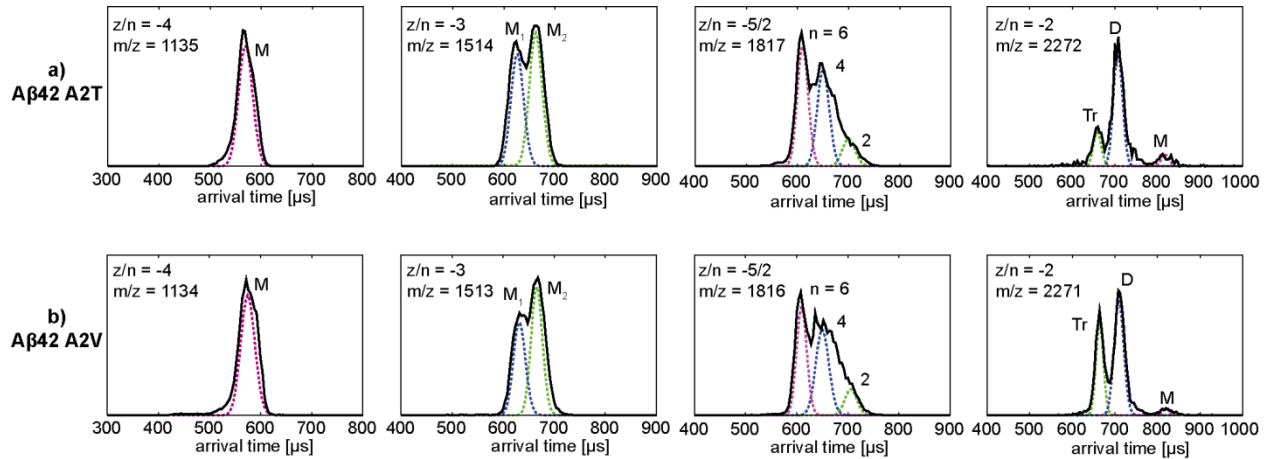


**Figure S6.** Ion mobility study of an equimolar mixture of *wt* and A2V A $\beta$ 40. a) mass spectrum of the A2V/*wt* A $\beta$ 40 mixture. b-d) ATDs of three  $-5/2$  oligomer peaks. The oligomer order ( $n$ ) is noted for each feature. The injection energy in panels b, c, and d is 40 eV.

### Summary of ion mobility studies of A $\beta$ 42 alloforms

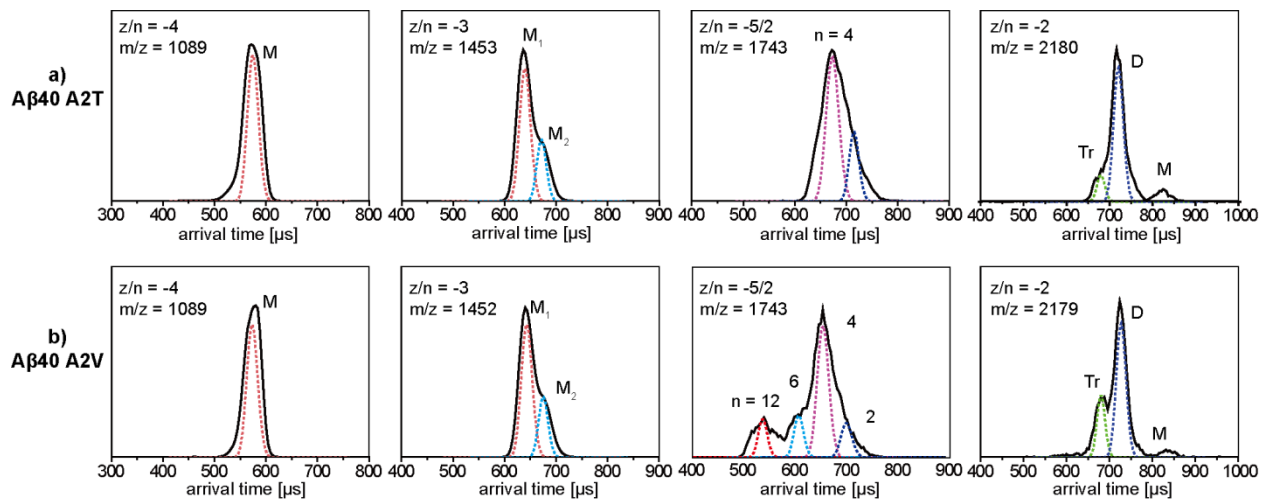


c) Cross sections for A $\beta$ 42 alloforms,  $\text{\AA}^2$

Oligomer	Charge State	Wild Type		A2T		A2V		A2T/ <i>wt</i>		A2V/ <i>wt</i>	
		$\sigma$	$\sigma/n$	$\sigma$	$\sigma/n$	$\sigma$	$\sigma/n$	$\sigma$	$\sigma/n$	$\sigma$	$\sigma/n$
Monomer	-2	-	-	624	623	620	620	-	-	-	-
	-3	643	643	647	647	645	645	-	-	-	-
	-3	702	702	706	706	704	704	-	-	-	-
	-4	792	792	791	791	801	801	-	-	-	-
Dimer	-4	-	-	934	467	954	477	944	472	952	476
	-5	1246	623	1224	612	1252	626	1258	629	1234	617
Trimer	-6	-	-	1227	409	1251	417	1239	413	1245	415
	-8	-	-	-	-	1749	583	-	-	-	-
Tetramer	-10	2172	543	2184	546	2216	554	2272	568	2272	568
Hexamer	-15	2838	473	2898	483	2946	491	2960	493	2934	489
	-16	-	-	-	-	3048	508	-	-	-	-
Dodecamer	-30	4560	380	-	-	-	-	-	-	-	-

**Figure S7.** ATDs of the  $z/n = -4, -3, -5/2$  and  $-2$  charge states for a) A2T and b) A2V A $\beta$ 42. The oligomer number ( $n$ ) is noted for each feature in the ATDs. The dashed lines represent the peak shape for a single conformation. The injection energy is 40 eV. c) Summary of cross sections values for A $\beta$ 42 alloforms and hetero-oligomers. The error (standard deviation) is within 1%.

## Summary of ion mobility studies of A $\beta$ 40 alloforms



c) Cross sections for A $\beta$ 40 alloforms,  $\text{\AA}^2$

Oligomer	Charge State	Wild Type		A2T		A2V		A2T/wt		A2V/wt	
		$\sigma$	$\sigma/n$	$\sigma$	$\sigma/n$	$\sigma$	$\sigma/n$	$\sigma$	$\sigma/n$	$\sigma$	$\sigma/n$
Monomer	-2	593	593	598	598	592	592	-	-	-	-
	-3	621	621	620	620	629	629	-	-	-	-
	-3	690	690	687	687	685	685	-	-	-	-
	-4	764	764	747	747	751	751	-	-	-	-
Dimer	-4	958	479	956	478	954	477	956	478	964	482
	-5	1160	580	1162	581	1226	613	1158	579	1162	581
Trimer	-6	-	-	1281	427	1272	424	1275	425	1269	423
Tetramer	-10	2084	521	2120	530	2164	541	2132	533	2136	534
Hexamer	-15	-	-	-	-	2922	487	-	-	-	-
Dodecamer	-30	-	-	-	-	4356	363	-	-	-	-

**Figure S8.** ATDs of the  $z/n = -4, -3, -5/2$  and  $-2$  charge states for a) A2T and b) A2V A $\beta$ 40. The oligomer number ( $n$ ) is noted for each feature in the ATDs. The dashed lines represent the peak shape for a single conformation. The injection energy is 40 eV. c) Summary of cross sections values for A $\beta$ 40 alloforms and hetero-oligomers. The error (standard deviation) is within 1%.

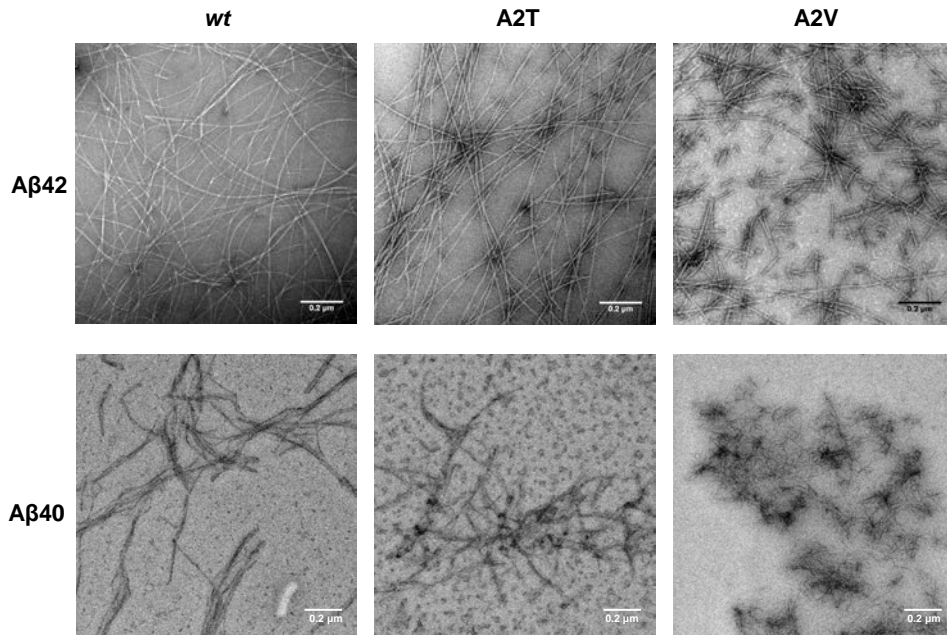


Figure S9. TEM images of Aβ samples after 5 days' incubation at room temperature. The scale bar is 200 nm.